Article

Journal of Vibration and Control
17(9) 1348–1358

DOI: 10.1177/1077546310378870
jvc.sagepub.com
SAGE

On the total variation of a third-order semi-discrete central scheme for 1D conservation laws

Mehdi Dehghan and Rooholah Jazlanian

Abstract

In this work, we present a third-order, semi-discrete, central-upwind scheme for computing approximate solutions of 1D systems of conservation laws. We combine the third-order CWENO reconstruction proposed in Levy et al., the semi-discrete central-upwind numerical flux proposed in Kurganov et al. and the third-order TVD Runge–Kutta method, proposed in Shu and Osher. We are interested in the behavior of the total variation of the approximate solution obtained with this scheme. Also we test our scheme on both scalar and gas dynamics problems. We observe that the total variation of computed solutions is close to the total variation of the exact solution or a reference solution.

Keywords

High-resolution, central schemes, hyperbolic conservation laws, total variation

Received: 1 November 2009; accepted: 24 June 2010

1. Introduction

High-resolution methods for solving systems of conservation laws

$$u_t + f(u)_x = 0 \quad u \in \mathbb{R}^{\mathrm{d}},\ \mathrm{d} \geq 1 \tag{1}$$

have attracted much attention over the past decade. Analytical solutions are available only in a very few special cases and numerical methods must be used in practical applications (Dehghan, 2005, 2006). There are two types of such methods, namely upwind schemes and central schemes.

In this work, we focus on the class of central schemes, i.e. schemes that can be implemented with very little knowledge of the structure of the system of conservation laws. Since the central schemes are Riemann-solver-free, these schemes are simple to implement, and can be extended to multi-dimensional problems.

Central-upwind schemes are semi-discrete variants of central schemes that have improved efficiency and less dissipation than fully-discrete central schemes. A second-order semi-discrete central scheme was introduced by Kurganov and Tadmor (2000). The basic idea in the construction of the second-order semi-discrete scheme was to use more accurate information about the local speed of propagation of the discontinuities. Modifications to this scheme, based on the one-sided local speed of propagation, were proposed by Kurganov et al. (2001). These schemes for the evolution step employ integration over Riemann fans and do not require a Riemann solver and characteristic decomposition,

Department of Applied Mathematics, Faculty of Mathematics and Computer Science, Amirkabir University of Technology, Iran

Corresponding author:
Mehdi Dehghan, Department of Applied Mathematics, Faculty of Mathematics and Computer Science, Amirkabir University of Technology, Tehran, Iran
Email: mdehghan@aut.ac.ir

so they are Godunov-type central schemes. Also, they have an upwind nature, since one-sided information is used to estimate the width of the Riemann fans.

In this work we use the numerical flux of Kurganov et al. (2001), which we refer to as the KNP flux. We combine the KNP flux with the third-order central weighted essentially non-oscillatory (CWENO) reconstruction of Levy et al. (2000b), and the third-order TVD Runge–Kutta method, proposed in Shu and Osher (1988).

In this paper, we investigate the question of the convergence of the semi-discrete central scheme for approximating solutions of hyperbolic systems of conservation laws. We numerically test the behavior of the total variation (TV), $TV(u) := \sum_j |u_{j+1} - u_j|$, of the discrete solution.

A scheme is called total variation bounded (TVB) in $0 \le t \le T$, if $TV(u^n) \le K$ for fixed positive K (constant K depends only on the initial condition), and $\forall n$, Δt s.t. $n\Delta t \le T$. If $TV(u^{n+1}) \le TV(u^n)$ then the scheme is total variation diminishing (TVD). If a scheme is TVB, then there exists a convergent subsequence in L^1_{LOC} to a weak solution of equation 1, which turns into strong convergence if an additional entropy condition is satisfied (see LeVeque, 1992, for more details). Our numerical results suggest that our scheme is TVB, which provides evidence of the convergence of the scheme.

This paper is organized as follows: in Section 2 we present our third-order central-upwind scheme. For that, we give a brief overview of the derivation of the KNP flux in Section 2.1. The third-order CWENO reconstruction is summarized in Section 2.2. Next, in Section 3 we present the results of a number of numerical tests of our scheme. We test both the accuracy and the evolution of the total variation of the resulting approximations. Finally, Section 4 ends this paper with a brief summary.

2. Third-order semi-discrete scheme

In this section we give a brief overview of the components that we use to construct our third-order central-upwind scheme: the numerical flux from Kurganov et al. (2001) and the reconstruction from Levy et al. (2000b). The problem is required to be hyperbolic, i.e. the flux Jacobian

$$A = \frac{\partial f(u)}{\partial u} \tag{2}$$

is required to have both real eigenvalues, $\lambda_1 \le \lambda_2 \le \cdots \le \lambda_N$, and a complete set of eigenvectors. If the real eigenvalues are distinct then the problem is strictly hyperbolic and a complete set of eigenvectors is guaranteed.

2.1. The KNP flux

Consider a uniform spatial grid where the cell $I_j = [x_{j-\frac{1}{2}}, x_{j+\frac{1}{2}}]$ has a width, h. Let the approximation to the cell average of u on I_j be given by $\bar{u}_j^n = \frac{1}{h}\int_{I_j} u(x, t^n)dx$. We assume that the cell averages $\{\bar{u}_j^n\}$ are known at time t^n. Let $\chi_j(x)$ be the characteristic function of the cell I_j. First, from $\{\bar{u}_j^n\}$, we reconstruct a piecewise polynomial $\tilde{u}(x, t^n) := \sum_j P_j(x)\chi_j(x)$. Here, $P_j(x)$ are polynomials of a suitable degree. We denote the point-values of $\tilde{u}(x, t^n)$ at the interfaces of the cell I_j by $u^+_{j+\frac{1}{2}} := P_{j+1}(x_{j+\frac{1}{2}})$ and $u^-_{j+\frac{1}{2}} := P_j(x_{j+\frac{1}{2}})$. The left- and right-sided local speeds of propagation of information from the discontinuities at the cell interfaces, $a^1_{j+\frac{1}{2}}$ and $a^N_{j+\frac{1}{2}}$, are estimated by

$$a^N_{j+\frac{1}{2}} = \max\left[\lambda_N\left(\frac{\partial f}{\partial u}\left(u^-_{j+\frac{1}{2}}\right)\right), \lambda_N\left(\frac{\partial f}{\partial u}\left(u^+_{j+\frac{1}{2}}\right)\right), 0\right] \tag{3}$$

and

$$a^1_{j+\frac{1}{2}} = \min\left[\lambda_1\left(\frac{\partial f}{\partial u}\left(u^-_{j+\frac{1}{2}}\right)\right), \lambda_1\left(\frac{\partial f}{\partial u}\left(u^+_{j+\frac{1}{2}}\right)\right), 0\right] \tag{4}$$

These local speeds of propagation are used to determine intervals for averaging that contain the Riemann fans from the cell interfaces. For more details see Kurganov et al. (2001).

One-dimensional grid updates of the average conserved variables are calculated using a conservative update as

$$\frac{d}{dt}\bar{u}_j(t) = -\frac{H_{j+\frac{1}{2}} - H_{j-\frac{1}{2}}}{h} \tag{5}$$

The numerical flux (KNP) in equation 5 is given by

$$H_{j+\frac{1}{2}} = \frac{a^N_{j+\frac{1}{2}} f\left(u^-_{j+\frac{1}{2}}\right) - a^1_{j+\frac{1}{2}} f\left(u^+_{j+\frac{1}{2}}\right)}{a^N_{j+\frac{1}{2}} - a^1_{j+\frac{1}{2}}} + \frac{a^N_{j+\frac{1}{2}} a^1_{j+\frac{1}{2}}}{a^N_{j+\frac{1}{2}} - a^1_{j+\frac{1}{2}}}\left(u^+_{j+\frac{1}{2}} - u^-_{j+\frac{1}{2}}\right) \tag{6}$$

The accuracy of this scheme is determined by the accuracy of the reconstructions and the ODE solver.

2.2. The third-order CWENO reconstruction

In the framework of upwind schemes, high-order essentially non-oscillatory (ENO) reconstructions were proposed in Harten et al. (1987). ENO schemes choose the stencil that provides the least oscillatory reconstruction. Weighted essentially non-oscillatory (WENO) reconstructions were described by Liu et al. (1994). Later, Jiang and Shu (1996) described improved smoothness indicators and efficient implementations of WENO schemes. In Bianco et al. (1999) high-order ENO reconstructions were first combined with central schemes. A new central WENO (CWENO) reconstruction for 1D hyperbolic conservation laws was proposed by Levy et al. (1999).

In each cell, I_j, we use a quadratic polynomial as a convex combination of three polynomials $P_L(x)$, $P_R(x)$ and $P_C(x)$,

$$P_j(x) = w_L P_L(x) + w_C P_C(x) + w_R P_R(x), \quad w_i \geq 0 \quad \forall i \in \{L, C, R\}, \quad \sum_i w_i = 1 \tag{7}$$

The linear functions, $P_R(x)$ and $P_L(x)$, are uniquely determined by requiring them to conserve the one-sided cell-averages ($\bar{u}_j^n$, $\bar{u}_{j+1}^n$ and $\bar{u}_j^n$, $\bar{u}_{j-1}^n$, respectively) as

$$P_R(x) = \bar{u}_j^n + \frac{\bar{u}_{j+1}^n - \bar{u}_j^n}{h}(x - x_j), P_L(x) = \bar{u}_j^n + \frac{\bar{u}_j^n - \bar{u}_{j-1}^n}{h}(x - x_j) \tag{8}$$

Also, $P_C(x)$ is chosen such that,

$$P_{opt}(x) = C_L P_L(x) + C_R P_R(x) + (1 - C_L - C_R) P_C(x) \tag{9}$$

with constants C_i's. Here, $P_{opt}(x) = u_j^n + u_j'(x - x_j) + \frac{1}{2}u_j''(x - x_j)^2$, is the parabola polynomial that interpolates the data, $\bar{u}_{j-1}^n$, $\bar{u}_j^n$ and $\bar{u}_{j+1}^n$, in the sense of cell-averages to enforce conservation

$$\int_{x_{j+l-\frac{1}{2}}}^{x_{j+l+\frac{1}{2}}} P_{opt}(x)dx = h\bar{u}_{j+l}^n, \quad l = -1, 0, 1$$

These conditions determine $P_{opt}(x)$ uniquely. In Levy et al. (2000b) it was shown that every symmetric selection of the constants C_i's in equation 9 will provide the desired third-order accuracy. In particular by taking $C_L = C_R = 1/4$, we obtain

$$P_C(x) = \bar{u}_j^n - \frac{1}{12}(\bar{u}_{j+1}^n - 2\bar{u}_j^n + \bar{u}_{j-1}^n) + \frac{\bar{u}_{j+1}^n - \bar{u}_{j-1}^n}{2h}(x - x_j) + \frac{\bar{u}_{j+1}^n - 2\bar{u}_j^n + \bar{u}_{j-1}^n}{h^2}(x - x_j)^2$$

As is said in Levy et al. (2000b), in smooth regions, the coefficients, w_i, of the convex combination in equation 7 are chosen to guarantee the maximum order of accuracy (in this particular case, order three), but in the presence of a discontinuity they are automatically switched to the best one-sided stencil (which generates the least oscillatory reconstruction). The weights are taken as

$$w_i = \frac{\alpha_i}{\sum_m \alpha_m}, \quad \alpha_i = \frac{C_i}{(\epsilon + IS_i)^2}, \quad i, m \in \{L, C, R\}$$

The constant, ϵ, guarantees that the denominator does not vanish and is taken as $\epsilon = 10^{-6}$. Also, the smoothness indicators, IS_i, are defined as

$$IS_i = \sum_{l=1}^{2} \int_{x_{j-\frac{1}{2}}}^{x_{j+\frac{1}{2}}} h^{2l-1}(P_i^{(l)}(x))^2 dx$$

A direct computation then results in

$$IS_L = \left(\bar{u}_j^n - \bar{u}_{j-1}^n\right)^2, \quad IS_R = \left(\bar{u}_{j+1}^n - \bar{u}_j^n\right)^2$$

$$IS_C = \frac{13}{3}\left(\bar{u}_{j+1}^n - 2\bar{u}_j^n + \bar{u}_{j-1}^n\right)^2 + \frac{1}{4}\left(\bar{u}_{j+1}^n - \bar{u}_{j-1}^n\right)^2$$

We refer the interested reader to references Bryson and Levy (2006), Bryson and Levy (2003), Kurganov and Levy (2000), Kurganov and Petrova (2001), Levy et al. (2000a), Nessyahu and Tadmor (1990), Peer et al. (2008), for more research works on one-dimensional conservation laws.

3. Numerical results

In this section, we describe the results of numerical examples for various test problems. We abbreviate our third-order semi-discrete scheme by SDS3, also we compare results with CCWENO (Compact Central Weighted Essentially Non-oscillatory) (Levy et al., 2000b). We test the accuracy of the scheme on problems with smooth solutions and solve various equations that admit non-smooth solutions. We also test the TV of the numerical experiments. To integrate equation 5 forward in time, we use the third-order TVD

Table 1. Errors and orders of convergence for advection equation at T = 1

N	L_1 error	L_1 order	L_∞ error	L_∞ order
40	4.0700(-2)	—	2.5700(-2)	—
80	1.1300(-2)	1.8487	1.0900(-2)	1.2374
160	2.2000(-3)	2.3607	3.4000(-3)	1.6807
320	1.7945(-4)	3.6158	4.7165(-4)	2.8497
640	9.2396(-6)	4.2796	2.2673(-5)	4.3787
1280	5.3421(-7)	4.1124	7.2460(-7)	4.9676

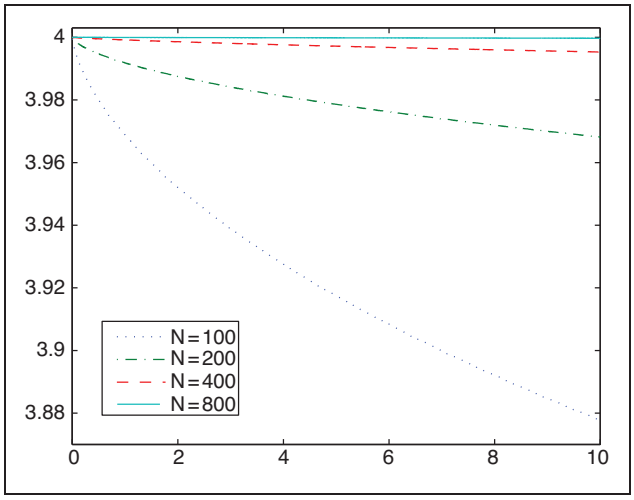

Figure 1. TV of the solution to a linear advection problem at T = 10.

Table 2. Errors and orders of convergence for Burgers' equation at T = 0.5

N	L_1 error	L_1 order	L_∞ error	L_∞ order
40	5.5300(-2)	—	6.1100(-2)	—
80	2.0900(-2)	1.4038	1.6400(-2)	1.8975
160	6.3000(-3)	1.7301	3.5000(-3)	2.2283
320	6.2883(-4)	3.3246	1.7548(-4)	4.3180
640	3.3923(-5)	4.2123	9.9539(-6)	4.1399
1280	1.1470(-6)	4.8863	1.3475(-6)	2.8850

Runge–Kutta method. In all of the numerical experiments below, the Courant-Friedrich-Levy (CFL) number is equal to 0.425.

3.1. Scalar test problems

We first consider the scalar linear hyperbolic equation

$$u_t + u_x = 0, \quad x \in [0, 2\pi]$$

augmented with the smooth initial data, $u(x, 0) = \sin(x)$, and periodic boundary conditions. The relative L_1- and $L_\infty-$ norms of the errors are shown in Table 1.

Note that the TV of the exact solution equals 4, and remains constant along the evolution. Figure 1 presents the TV of the semi-discrete approximate solution, which is computed using the point-values obtained with the CWENO reconstruction from the cell-averages.

Next, we consider the initial boundary value problem (IBVP) for the inviscid Burgers' equation

$$u_t + \left(\frac{u^2}{2}\right)_x = 0, \quad u(x, 0) = 2 - \cos(x), \quad x \in [0, 2\pi]$$

with periodic boundary conditions. We test the accuracy at $T = 0.5$ (before shock formation), and the results are shown in Table 2.

Figure 2 shows the solution after shock formation at $T = 3$, and the change in the TV of the approximation for different cells compared with the TV of the exact solution. The TVs of the approximate solutions have the same behavior as the TV of the exact solution. The values of the TV of the approximate solutions never increase above the exact TV. We also observe that the TVs of the approximate solutions are different from that of the exact solution for two reasons: (a) the TV is computed on a discrete set of points, (b) the discrete values of the numerical solution are not exact.

Our next example is Burgers' equation on the same domain with initial data, $u(x, 0) = 2 + \cos(x) - \cos(2x)$. This example develops two shocks, which eventually merge. Figure 3 shows the solution after shock formation at $T = 1.2$, and the change in the TV of the approximation for different cells compared with the TV of the exact solution.

3.2. Systems of conservation laws

In this subsection we use the third-order semi-discrete scheme to solve hyperbolic systems of conservation laws. In particular, we solve the Euler equations of gas dynamics for a polytropic gas

$$\frac{\partial}{\partial t}\begin{pmatrix}\rho\\ \rho q\\ E\end{pmatrix} + \frac{\partial}{\partial x}\begin{pmatrix}\rho q\\ \rho q^2 + p\\ q(E+p)\end{pmatrix} = 0, \quad p = (\gamma - 1)(E - \frac{1}{2}\rho q^2),$$
$$\gamma = 1.4 \tag{10}$$

We first use third-order semi-discrete scheme for the Sod problem proposed in Sod (1978) on the domain [0, 1] with initial data

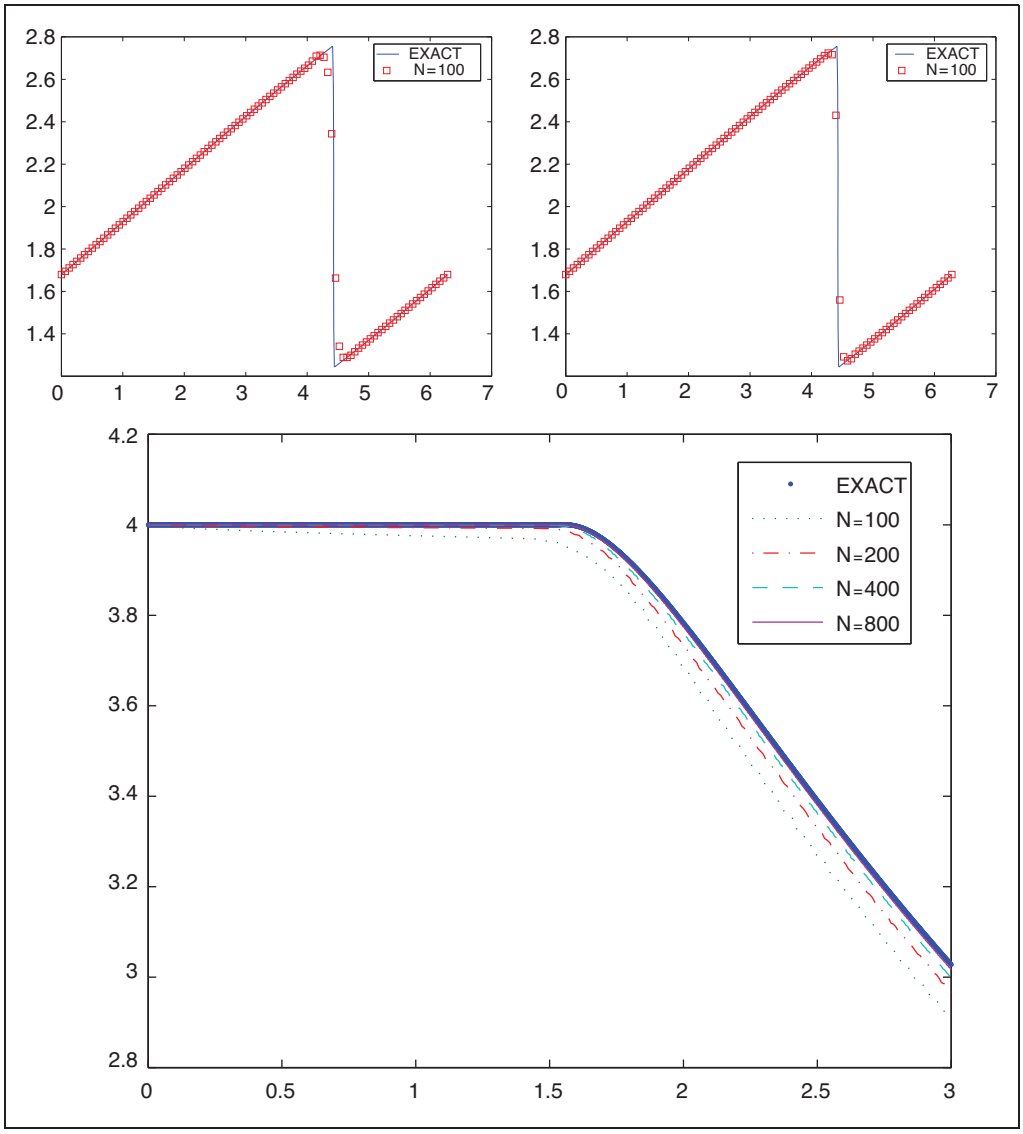

Figure 2. Results for the Burgers' equation. Top: the solution after shock formation at $T = 3$ (left: SDS3, right: CCWENO). Bottom: the change in the TV of the approximation for different cells (left to right) compared with the TV of the exact solution.

$$u(x,0) = \begin{cases} (1,0,2.5)^T & 0 \le x < 0.5 \\ (0.125,0,0.25)^T & 0.5 \le x \le 1 \end{cases}$$

Figure 4 shows the performance of SDS3 and CCWENO at $T = 0.16$ with $N = 200$. Also, Figure 4 shows the TV behavior of the approximation, compared with a reference solution. We observe that the shock and the contact discontinuity are well captured at low resolution. We also see that the TVs of the approximate solutions are initially greater than that of the reference solution, but converge to the TV of the reference solution over time.

Next, we apply SDS3 and CCWENO to the Lax problem. In this test, which is taken from Lax (1954), we solve equation 10 with the initial condition

$$u(x,0) = \begin{cases} (0.445, 0.31061, 8.92840289)^T & 0 \le x < 0.5, \\ (0.5,0,1.4275)^T & 0.5 \le x \le 1, \end{cases}$$
$$x \in [0,1]$$

For this more difficult shock tube problem, Figure 5 shows the performance of our scheme and CCWENO at $T = 0.16$ with $N = 200$. Similar to Sod's test problem, the shock and the contact discontinuity are well

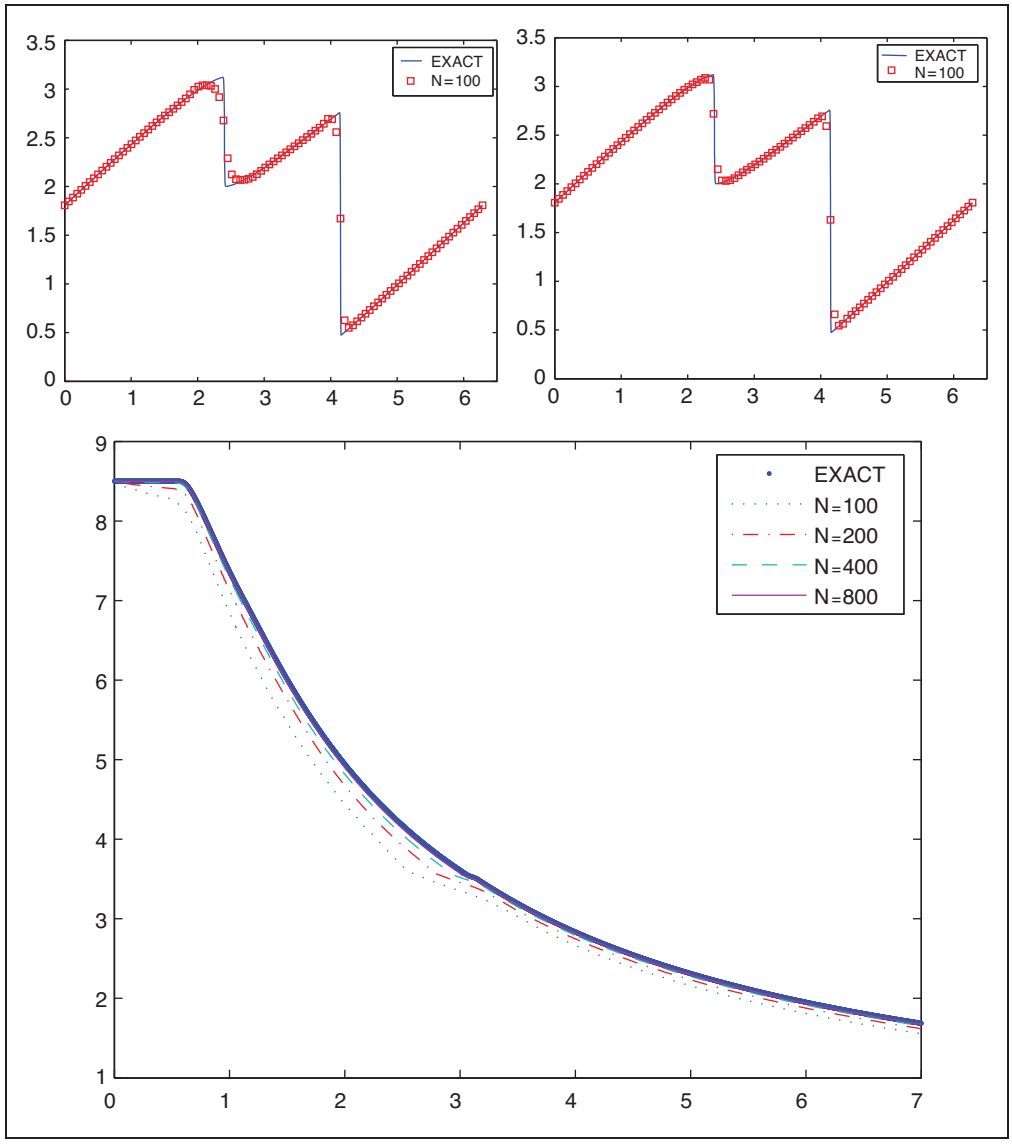

Figure 3. Results for the 2-shock Burgers' problem. Top: the solution after shock formation at $T = 1.2$ (left: SDS3, right: CCWENO). Bottom: the change in the TV of the approximation for different cells (left to right) compared with the TV of the exact solution.

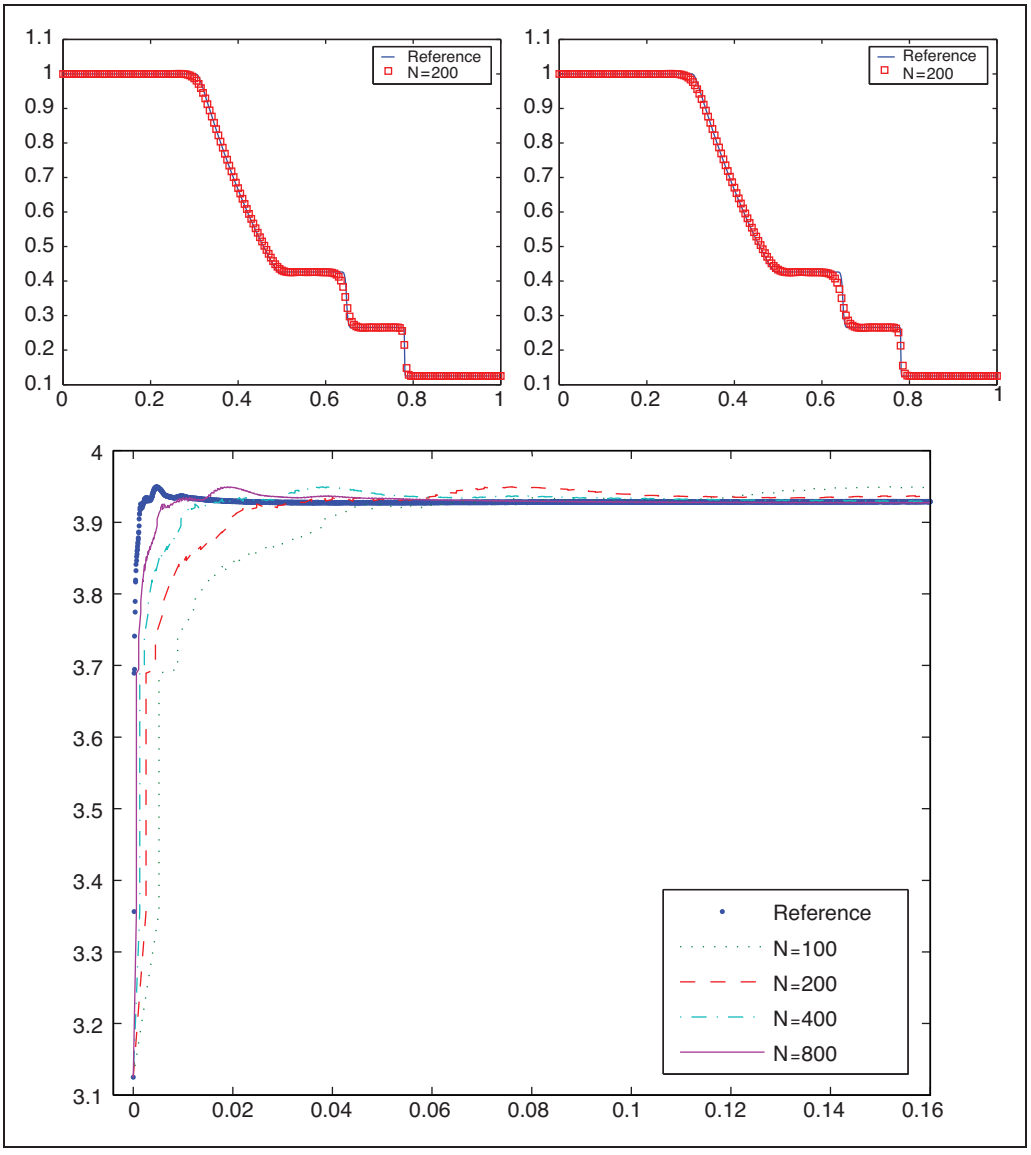

Figure 4. Results for the Sod problem. Top: the density profile at $T = 0.16$ (left: SDS3, right: CCWENO). Bottom: the change in the TV of the approximation for different cells compared with the TV of a reference solution.

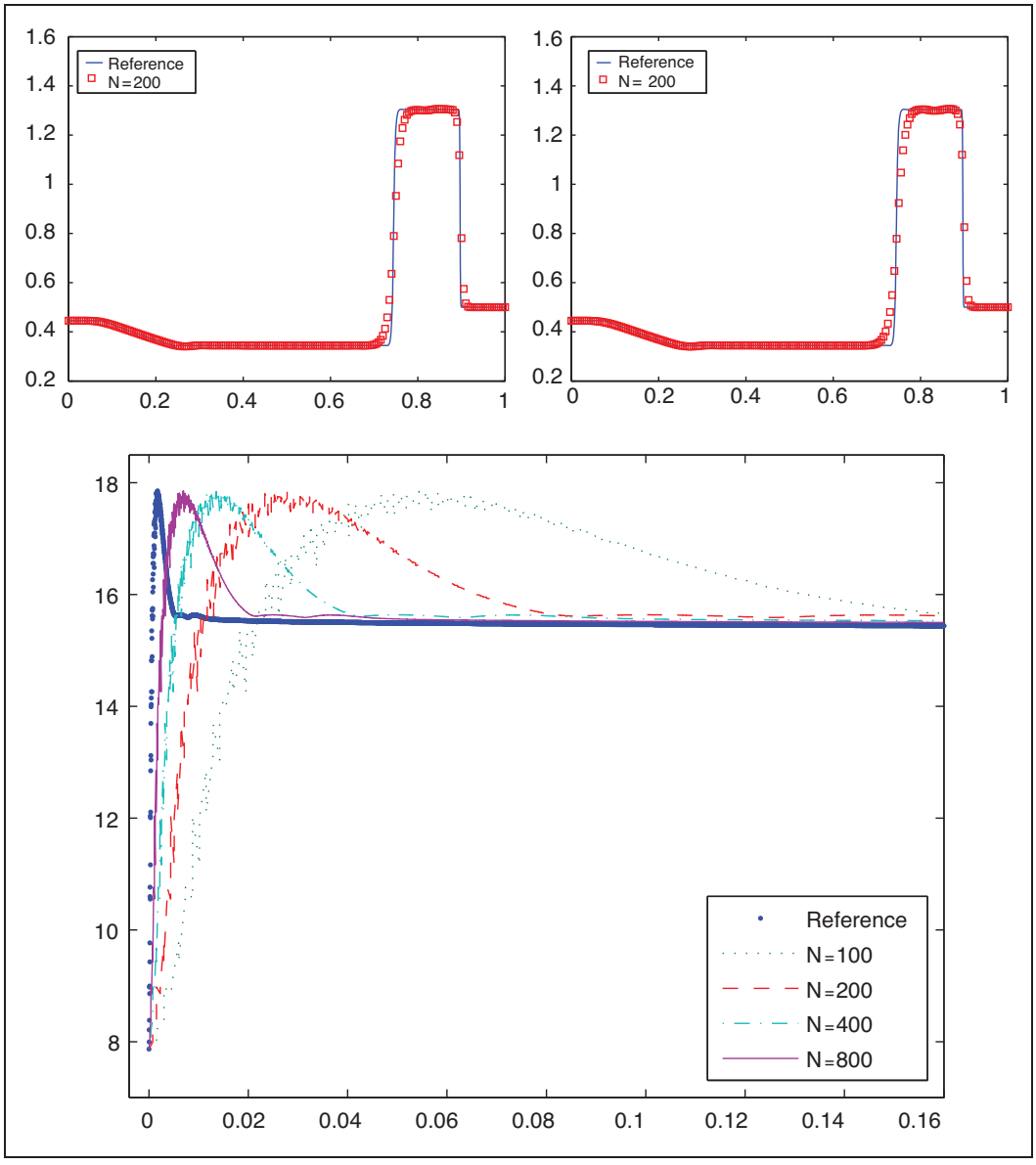

Figure 5. Results for the Lax problem. Top: the density profile at $T = 0.16$ (left: SDS3, right: CCWENO). Bottom: the change in the TV of the approximation for different cells compared with the TV of a reference solution.

captured at low resolution, but there are significant oscillations between the contact discontinuity and the shock for $N = 100$. The high-order schemes clearly exhibit small amplitude spurious oscillations in this test problem. These oscillations are of the ENO type, in the sense that their amplitude decreases as the grid is refined. We see that the TVs of the approximate solutions are initially greater than that of the reference solution, but similar to the Sod problem, converge to the TV of the reference solution over time. It is interesting, however, that the over-shoot of the TV at early times does not seem to depend on the mesh resolution.

For the next example, which is taken from Woodward and Colella (1984), we solve the Euler equations 10 with a shock interaction problem with solid wall boundary conditions, applied to both ends given by the initial data

$$u(x,0) = \begin{cases} (1,0,2500)^T & 0 \le x < 0.1 \\ (1,0,0.025)^T & 0.1 \le x < 0.9 \\ (1,0,250)^T & 0.9 \le x \le 1 \end{cases}$$

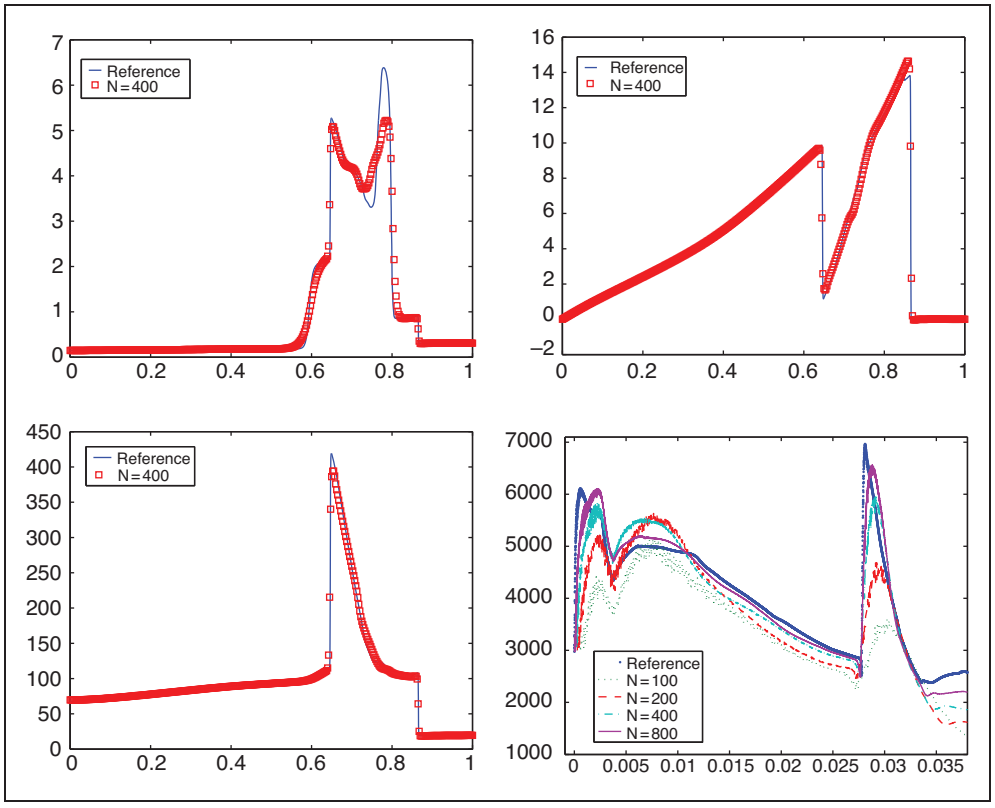

Figure 6. Results for the Woodward–Colella problem. Top left: the density profile and right: the velocity profile at $T=0.038$. Bottom left: the pressure profile at $T=0.038$ and right: the change in the TV of the approximation for different cells compared with the TV of a reference solution.

on the domain $x\in[0,\ 1]$. We display the numerical results of the density, velocity and pressure profile of this complex problem in Figure 6. The results are with $N=400$ at $T=0.038$, and we get a reference solution using 4000 cells. We observe some numerical oscillations. Figure 6 also shows the TV behavior of the approximation, compared with the reference solution. We also see that the TVs of the numerical solutions converge to the TV of the reference solution, but do not seem to converge over time. This is not surprising since this example contains sharp peaks that will not be resolved for coarse meshes.

For the final test, which is taken from Shu and Osher (1988), we solve the Euler equations 10 with a moving Mach = 3 shock interacting with sine waves in density, i.e.

$$u(x,0)=\begin{cases}(3.85714,\ 10.1418096304,\ 39.16655928489427)^T & -5\le x<\ -4\\ (1+0.2\sin(5x),\ 0,\ 2.5)^T & -4\le x\le 5\end{cases}$$

The flow contains physical oscillations that have to be resolved by the numerical method. We compute the solution at $T=1.8$. We show the numerical approximations of the density profile in Figure 7 along with a reference solution computed with 5000 cells. Figure 7 also displays the TV behavior of the approximation, compared with the reference solution. Numerical approximations of the density profile show the performance of the scheme in smooth regions and the ability to capture shocks. We also observe that the TV of our approximations converges to that of the reference solution.

4. Conclusion

In this work, we have introduced a third-order, semi-discrete, central-upwind scheme for computing

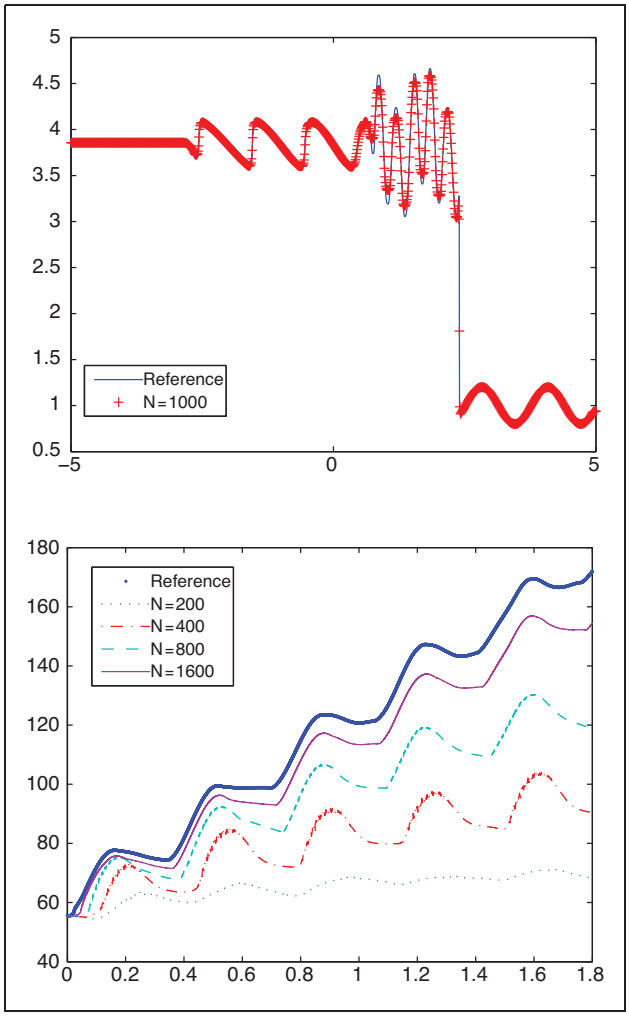

Figure 7. Results for the Shock-Entrop problem. Top: the density profile at $T = 1.8$. Bottom: the change in the TV of the approximation for different cells compared with the TV of a reference solution.

approximate solutions of 1D systems of conservation laws. First, we would like to comment that this scheme can be easily generalized to 2D problems. Also, we checked the behavior of the TV of the approximate solution obtained with this scheme and observed that the TV of a numerical solution for the third-order semi-discrete scheme is bounded for the test cases considered. In particular, we applied this scheme to solve Euler equations of gas dynamics. We observed that the TV approaches the TV of the reference solution in various ways for various cases. For example, in the Shock-Entrop problem (Shu and Osher, 1988) it is monotone while in the Woodward–Colella problem it is not.

References

Bianco F, Puppo G and Russo G (1999) High-order central schemes for hyperbolic systems of conservation laws. *SIAM Journal on Scientific Computing* 21: 294–322.

Bryson S and Levy D (2003) High-order semi-discrete central-upwind schemes for multi-dimensional Hamilton-Jacobi equations. *Journal of Computational Physics* 189: 63–87.

Bryson S and Levy D (2006) On the total variation of high-order semi-discrete central schemes for conservation laws. *Journal of Scientific Computing* 27: 163–175.

Dehghan M (2005) On the solution of an initial-boundary value problem that combines Neumann and integral condition for the wave equation. *Numerical Methods for Partial Differential Equations* 21: 24–40.

Dehghan M (2006) Finite difference procedures for solving a problem arising in modeling and design of certain optoelectronic devices. *Mathematics and Computers in Simulation* 71: 16–30.

Harten A, Engquist B, Osher S and Chakravarthy S (1987) Uniformly high order accurate essentially non-oscillatory schemes III. *Journal of Computational Physics* 71: 231–303.

Jiang GS and Shu CW (1996) Efficient implementation of weighted ENO schemes. *Journal of Computational Physics* 126: 202–228.

Kurganov A and Levy D (2000) A third-order semi-discrete central scheme for conservation laws and convection-diffusion equations. *SIAM Journal on Scientific Computing* 22: 1461–1488.

Kurganov A and Petrova G (2001) A third-order semidiscrete genuinely multidimensional central scheme for hyperbolic conservation laws and related problems. *Numerische Mathematik* 88: 683–729.

Kurganov A and Tadmor E (2000) New high-resolution central schemes for non-linear conservation laws and convection-diffusion equations. *Journal of Computational Physics* 160: 241–282.

Kurganov A, Noelle S and Petrova G (2001) Semi-discrete central-upwind schemes for hyperbolic conservation laws and Hamilton–Jacobi equations. *SIAM Journal on Scientific Computing* 23: 707–740.

Lax PD (1954) Weak solutions of non-linear hyperbolic equations and their numerical computation. *Communications on Pure and Applied Mathematics* 7: 159–193.

LeVeque RJ (1992) Numerical Methods for Conservation Laws. *Lectures in Mathematics*. Basel: Birkhauser.

Levy D, Puppo G and Russo G (1999) Central WENO schemes for hyperbolic systems of conservation laws. *Mathematical Modelling and Numerical Analysis* 33: 547–571.

Levy D, Puppo G and Russo G (2000a) On the behavior of the total variation in CWENO methods for conservation laws. *Applied Numerical Mathematics* 33: 407–414.

Levy D, Puppo G and Russo G (2000b) Compact central WENO schemes for multidimensional conservation laws. *SIAM Journal on Scientific Computing* 22: 656–672.

Liu XD, Osher S and Chan T (1994) Weighted essentially non-oscillatory schemes. *Journal of Computational Physics* 115: 200–212.

Nessyahu H and Tadmor E (1990) Non-oscillatory central differencing for hyperbolic conservation laws. *Journal of Computational Physics* 87: 408–463.

Peer AAI, Gopaul A, Dauhoo MZ and Bhuruth M (2008) A new fourth-order non-oscillatory central scheme for

hyperbolic conservation laws. *Applied Numerical Mathematics* 58: 674–688.

Shu CW and Osher S (1988) Efficient implementation of essentially non-oscillatory shock-capturing schemes. *Journal of Computational Physics* 77: 439–471.

Sod G (1978) A survey of several finite difference methods for systems of non-linear hyperbolic conservation laws. *Journal of Computational Physics* 27: 1–31.

Woodward P and Colella P (1984) The numerical solution of two-dimensional fluid flow with strong shocks. *Journal of Computational Physics* 54: 115–173.